Physical characterization of functionalized spider silk: electronic and sensing properties

Supplementary data

1. Humidity-dependent conductivity measurement

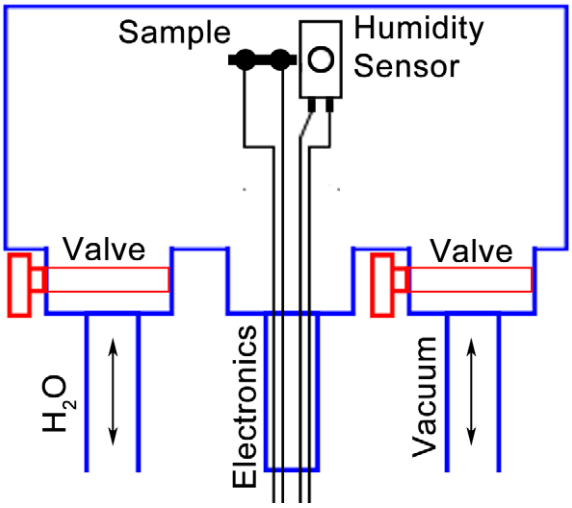

Figure S1. Schematic of the setup used for conductivity *vs. RH* measurements. Sample and humidity sensor (model HIH-5030-001 from Newark) were mounted side by side in the vacuum chamber through the middle opening. The left chamber was connected to the water reservoir. The right chamber was connected to a vacuum pump. *RH* was controlled by regulating the left and right valves.

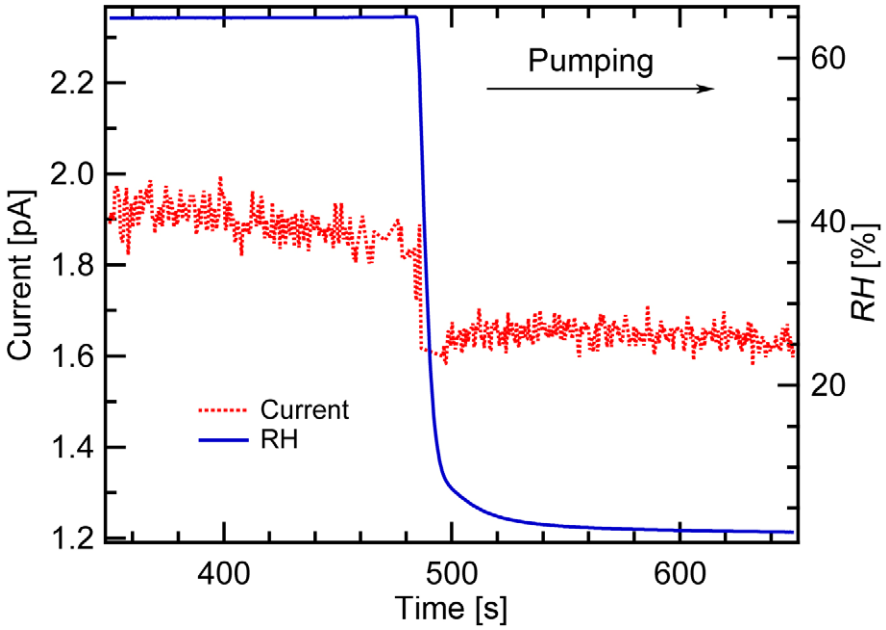

Figure S2. Background current check (with only electrical wires inside the chamber and no sample) in different *RH* (~65% and ~3%) level at an applied voltage of 20 V. The background current increase from ~3% to ~65% *RH* was very small (~1 pA) compared to the signal produced by the sample (for example, the neat spider silk). This background check is important because of the highly insulating nature of the neat silk fiber.

2. I-V measurement of neat silk

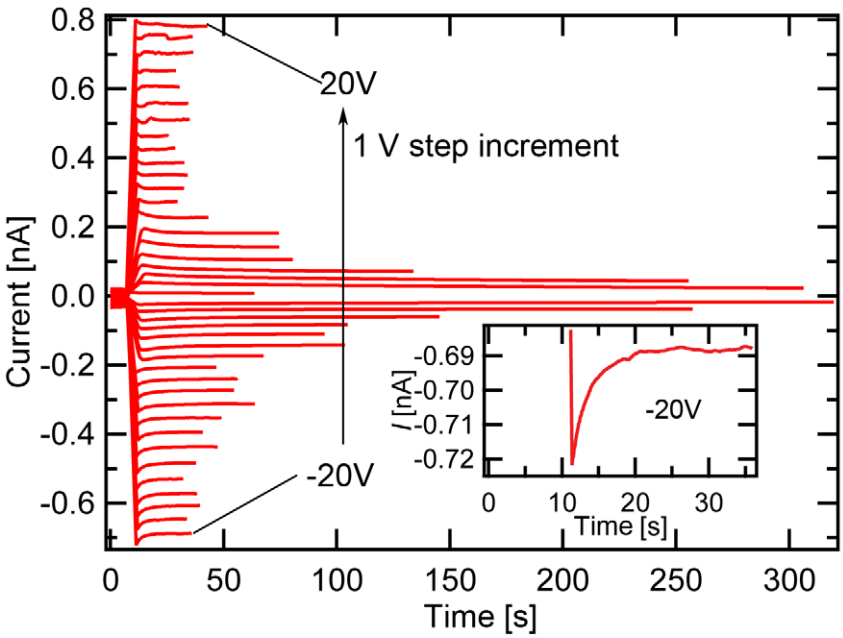

Figure S3. Current *vs*. time measurement of neat *P. phalangioides* silk fiber at constant voltages between -20 V (lowest curve) and 20 V (highest curve) with an increment of 1 V (for the intermediate curves). Inset: current vs. time curve at -20 V showing the approach to the steady state.

Because of the highly insulating nature of the neat silk fiber, it is very important to allow time for the discharge of any stray capacitance present in the system. Depending on the applied voltage, the time constant for this particular measurement ranged between ~3 min (for low voltages such as 1 V) and ~5 s (for high voltages such as 20 V). The data shown in figure 2a is derived from this measurement by plotting the current values for each voltage after reaching steady state.

3. Thermoelectric setup

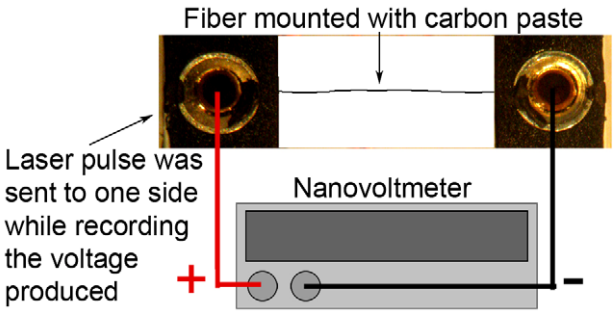

Figure S4. Room-temperature thermoelectric measurement setup. The fiber was mounted using carbon paste to the terminals of a standard integrated circuit 8-pin socket, and connected to a Keithley 1282 nanovoltmeter in a two-terminal configuration (the background image have been removed to show only the fiber). The heat pulse was generated at the terminal connection using a He-Ne laser (35 mW, 633 nm) to introduce the thermal gradient.

4. Measurement of gold-sputtered spider silk electrical junctions

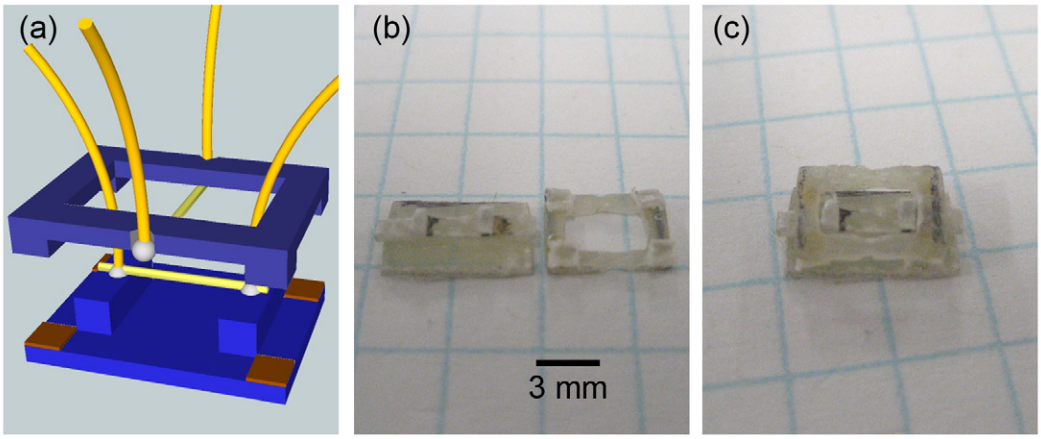

Figure S5. (a) Schematic of the junction configuration. Blue: substrate, brown: GE varnish, yellow: gold-sputtered silk fibers, white: silver paste, orange: gold wire. The gold-sputtered silk fiber was attached to the bottom and top substrates using silver paste. The two substrates were then pressed together and secured using GE varnish to make electronic junctions with tension between the two silk fibers. (b) Photograph of actual substrates before and after (c) assembly.

5. Mandolin method

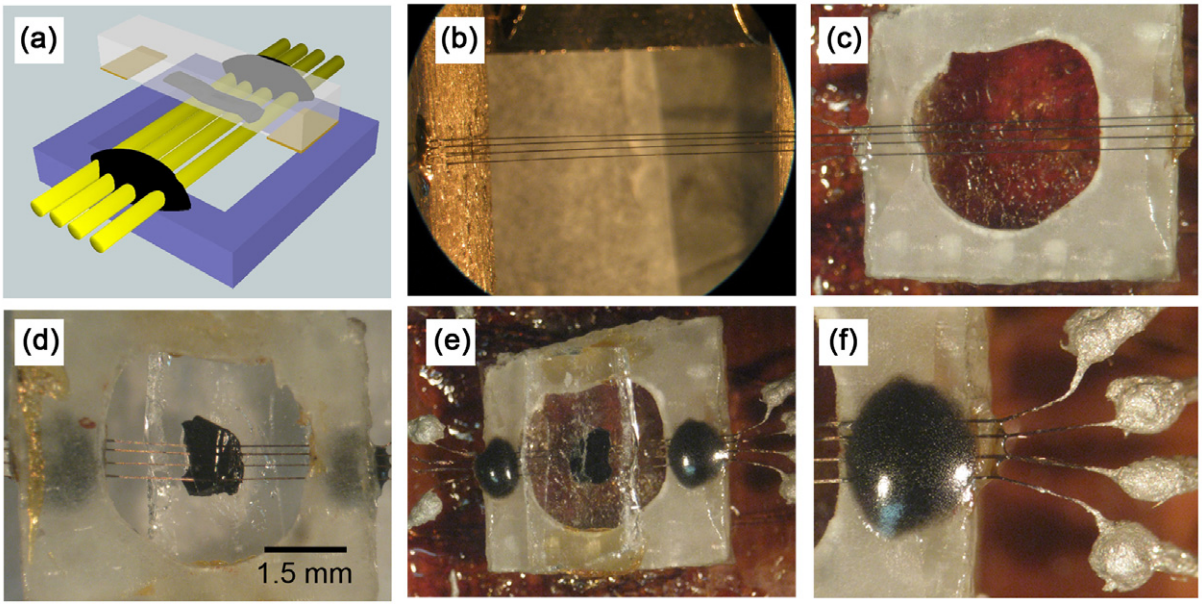

Figure S6. The mandolin method for performing four-probe electrical measurements using gold-coated spider fibers on organic samples. (a) Mandolin diagram. Blue: substrate, yellow: gold-sputtered silk fibers, black: Stycast 2850, brown: GE varnish, black rectangle: sample. (b) Four individual dragline silk fibers were first aligned on two toothpicks and secured using GE varnish, after which they were gold-sputtered for 2×30 seconds at current ~40 mA with a 15 seconds break in between. (c) The four aligned gold-sputtered silk fibers were transferred to a substrate by first placing the substrate on top of the aligned fibers, then gluing the two sides using GE varnish or enamel, and lastly, cutting the fibers. The fibers were further secured onto the substrate with Stycast 2850. (d) The sample was placed on a slide glass and then pressed against the aligned fibers manually under the microscope. The substrate and slide glass are secured by GE varnish. (e) The assembly is secured to a sample holder

where electrical contacts between the fibers and the copper wires can be made using silver paste. (f) The gold-sputtered silk fibers remained conducting even after considerable bending.

It is very important to secure the gold-sputtered silk fibers using the Stycast 2850 for low-temperature measurements. This prevents the fibers from slipping and losing the tension.

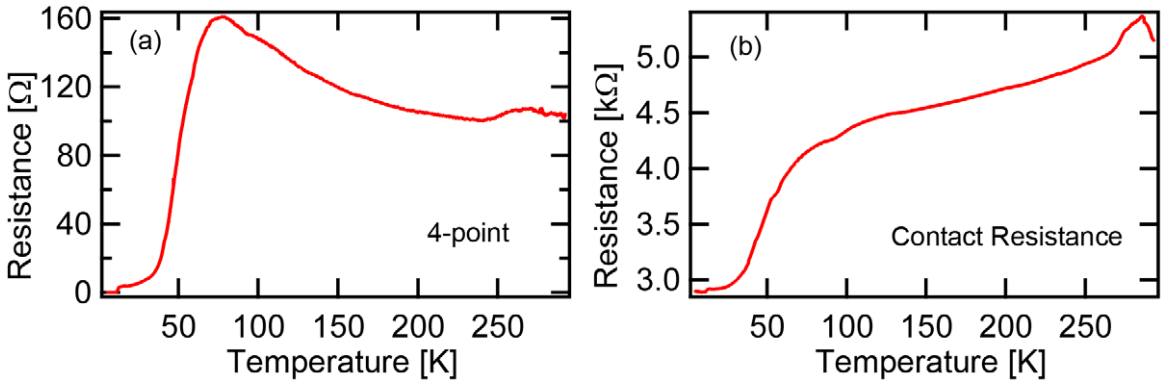

Figure S7. (a) Temperature-dependent four-terminal resistance of κ-(BEDT-TTF)$_2$Cu[N(CN)$_2$]Br measured using the mandolin technique from 300 to 4.3 K. (b) Temperature dependence of the contact resistance from 300 to 4.3 K. Here the resistances of the sample and the resistances of the connecting wires for a two-terminal configuration have been subtracted to show only the influence of the sample and of the wire contact resistance.

Measurements were very stable and robust down to ~4.3 K, and multiple cooling and warming cycles were carried out. In general, the contact resistance diminished at lower temperatures. There was however, a bump in the contact resistance data between 250 and 300 K, affecting the four-probe resistance measurement in this temperature range. The initial increase in the contact resistance might be due to differential cooling rates in different components of the mandolin assembly.

6. Amino acids appearing in the NMR spectra

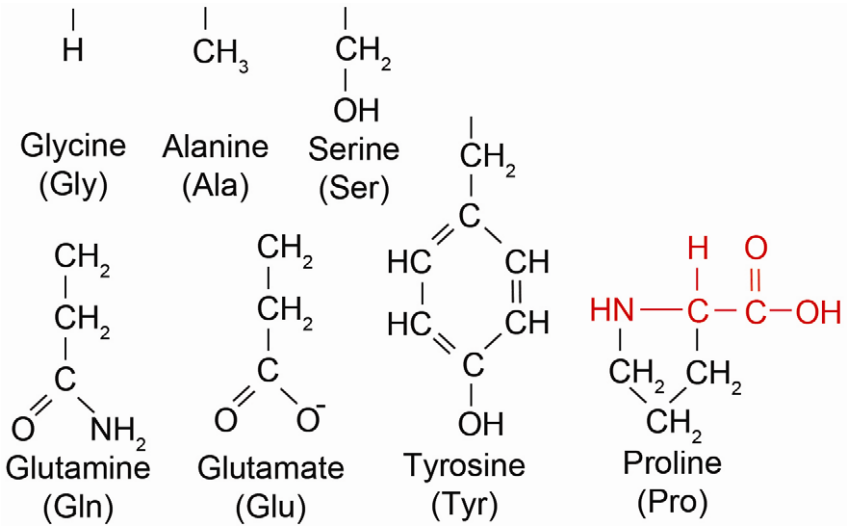

Figure S8. Structure of amino acids appearing in the NMR spectra. Glx used in the labeling of the NMR spectra corresponds to both glutamine (Gln) and glutamate (Glu). Red-labeled structure corresponds to a protein backbone segment.